Appl. Math. and Comp. Sci., 1998, Vol.8, No.1, 159–181

EVALUATION OF DISCRETE-TIME VSC ON AN INVERTED PENDULUM APPARATUS WITH ADDITIONAL DYNAMICS

MASAAKI HARA*, KATSUHISA FURUTA*
YAODONG PAN*, TASUKU HOSHINO*

Discrete-time Variable Structure Control (VSC) with sliding sector is experimentally evaluated on a new rotational-type inverted pendulum apparatus including an additional dynamics which is used to investigate the robustness of the controller. It is experimentally shown that the discrete-time VS controller makes the system robust stable with respect to parameter uncertainties and gives a quick response against external disturbances, which yields a good control performance without chattering.

1. Introduction

Continuous-time Variable Structure Control (VSC) with sliding mode is known to be robust with respect to parameter uncertainties and external disturbances. The sliding motion designed for a continuous-time system may not be satisfactorily achieved by VSC implemented in a discrete-time system. The robustness of the continuous-time VSC with sliding mode is not assured in the discrete-time system. A stable sliding mode designed in the continuous-time system may even become unstable under sampled-data control (Furuta and Pan, 1994).

To design VSC for discrete-time systems, a sliding sector was proposed in (Furuta, 1990; Furata and Pan, 1993; Iordanou and Surgenor, 1997) instead of the sliding mode. The control law of the discrete-time VSC transfers the system state from the outside to the inside of the sliding sector where the closed-loop system is designed to be stable.

The sliding sector inside which a norm of the system state decreases with zero input was first proposed in (Furuta and Pan, 1995), where sectors for both continuous-time and discrete-time systems were defined. Such a sliding sector exists for any controllable system. The sliding sector can be designed for a controllable canonical form or using a Riccati equation. The discrete-time VSC with sliding sector was designed to transfer the system state from the outside to the inside of the sliding sector while the norm is kept decreasing. The control system has been evaluated through the usual inverted pendulum. But the inverted pendulum could not include the uncertain dynamics model in the neighborhood of the equilibrium state.

* Department of Mechanical and Environmental Informatics, Tokyo Institute of Technology, 2–12–1, Oh-okayama, Meguro-ku, Tokyo 152, Japan, e-mail: mhara@ctrl.titech.ac.jp.

In this paper, a new rotational inverted pendulum is designed to have a mass, dumper and spring system between the rotational arm and hinge for the pendulum as an additional dynamics shown in Fig. 2. Assuming the additional dynamics to be an uncertainty, the robustness of the control system could be evaluated by using this experimental apparatus. The sliding sector is designed using the Riccati equation proposed in (Furuta and Pan, 1996) for the stabilizing controller of the proposed pendulum system.

The organization of the paper is as follows: Section 2 describes the sliding sector for a discrete-time system, designed via Riccati equation, and proposes a VS controller. Section 3 shows the experimental apparatus. Section 4 presents the results of experiments.

2. VSC with *PR*-Sliding Sector

Consider a single-input discrete-time plant:

$$x_{k+1} = \Phi x_k + \Gamma u_k \tag{1}$$

where $x_k \in \mathbb{R}^n$ and $u_k \in \mathbb{R}^1$ are the state and input vectors, respectively. Φ and Γ are constant matrices of appropriate dimensions, and the pair (A, B) is controllable.

2.1. *PR*-Sliding Sector

Definition 1. The *P-norm* $\|\cdot\|_p$ of the system state is defined as

$$\|x_k\|_p = (x_k^T P x_k)^{1/2}, \qquad x_k \in \mathbb{R}^n \tag{2}$$

where $P \in \mathbb{R}^{n\times n}$ is a positive-definite symmetric matrix.

If the autonomous system (1) is stable, then

$$L_{k+1} - L_k = x_k^T(\Phi^T P \Phi - P)x_k \leq 0, \qquad \forall x_k \in \mathbb{R}^n \tag{3}$$

for some positive-definite symmetric matrix $P \in \mathbb{R}^{n\times n}$, where L_k is defined as

$$L_k = \|x_k\|_p^2$$

But for an unstable system, inequality (3) does not hold. It is still possible that $L_{k+1} - L_k > 0$ for some $x_k \in \mathbb{R}^n$, and $L_{k+1} - L_k \leq 0$ for the other $x_k \in \mathbb{R}^n$. The latter ones form a subset in which the P-norm $\|x_k\|_p$ decreases. Accordingly, we define the subset called the PR-sliding sector as follows.

Definition 2. The *PR-sliding sector* is the subset of $\mathbb{R}^n$ defined as

$$\mathcal{S} = \left\{ x_k \middle|\ x_k^T(\Phi^T P \Phi - P)x_k \leq -x_k^T R x_k \right\} \tag{4}$$

where $P \in \mathbb{R}^{n\times n}$ is a positive-definite symmetric matrix and $R \in \mathbb{R}^{n\times n}$ is a positive semi-definite symmetric matrix.

Inside the PR-sliding sector, the P-norm $\|x_k\|_p$ of the plant (1) with zero control action does not increase because

$$L_{k+1} - L_k \leq -x_k^T R x_k \leq 0, \qquad \forall x_k \in \mathcal{S} \tag{5}$$

The existence of such a sliding sector for the discrete-time plant (1) is guaranteed by the following theorem.

Theorem 1. *For the plant (1), the PR-sliding sector defined by (4) exists for any positive-definite symmetric matrix P and any positive semi-definite symmetric matrix R. It can be rewritten as*

$$\mathcal{S} = \left\{ x_k \middle| \ s_k^2 \leq \delta_k^2 \right\} \tag{6}$$

where

$$s_k^2 = x_k^T P_1 x_k \geq 0 \tag{7}$$

$$\delta_k^2 = x_k^T P_2 x_k \geq 0 \tag{8}$$

P_1 and P_2 are $n \times n$ positive semi-definite symmetric matrices.

Proof. Set

$$\Delta = \Phi^T P \Phi - P + R \tag{9}$$

Then the PR-sliding sector defined by (4) is determined by the condition

$$x_k^T \Delta x_k \leq 0$$

For the matrix Δ, there exists a real orthonormal matrix $U \in \mathbb{R}^{n \times n}$ such that

$$U^T \Delta U = \operatorname{diag}(r_1, r_2, \ldots, r_n)$$

where r_i $(i = 1, 2, \ldots, n)$ are the characteristic roots of Δ, which are all real because Δ is symmetric.

Assume

$$\bar{P}_1 = \operatorname{diag}\left(\frac{|r_1| + r_1}{2}, \frac{|r_2| + r_2}{2}, \ldots, \frac{|r_n| + r_n}{2} \right)$$

$$\bar{P}_2 = \operatorname{diag}\left(\frac{|r_1| - r_1}{2}, \frac{|r_2| - r_2}{2}, \ldots, \frac{|r_n| - r_n}{2} \right)$$

i.e. $\bar{P}_1$ and $\bar{P}_2$ are composed of the positive and negative eigenvalues of Δ, respectively. Then we have

$$U^T \Delta U = \bar{P}_1 - \bar{P}_2$$

$$\bar{P}_i \geq 0, \qquad (i = 1, 2)$$

Introducing $P_i = U\bar{P}_i U^T \quad (n = 1, 2)$ gives

$$\Delta = P_1 - P_2$$

$$P_i \geq 0, \qquad (i = 1, 2)$$

The PR-sliding sector defined by (4) can thus be rewritten as

$$\mathcal{S} = \left\{ x_k \middle| \ s_k^2 \leq \delta_k^2 \right\}$$

where

$$s_k^2 = x_k^T P_1 x_k \geq 0$$

$$\delta_k^2 = x_k^T P_2 x_k \geq 0$$

which implies the existence of the PR-sliding sector. ■

Corollary 1. *Let $n_i = \mathrm{rank}(P_i)$ $(i = 1, 2)$ and $n_3 = n - n_1 - n_2$. Then n_1 and n_2 are the numbers of the positive and negative eigenvalues of Δ, respectively, and n_3 is the number of the eigenvalues of Δ at the origin.*

Remark 1. There are some special PR-sliding sectors:

- The PR-sliding sector $\mathcal{S}$ is equal to $\mathbb{R}^n$ if $n_1 = 0$.
- The PR-sliding sector $\mathcal{S}$ is reduced to the PR-sliding hyperplane determined by $x^T P_1 x = 0$ if $n_2 = 0$ and $n - n_1 > 0$.
- The PR-sliding sector $\mathcal{S}$ is reduced to the equilibrium point $x = 0$ if $n_1 = n$.

If $\mathrm{rank}(P_1) = 1$, the PR-sliding sector defined by (6) has a simplified form

$$\mathcal{S} = \left\{ x_k \middle| \ |s_k| \leq |\delta_k| \right\} \tag{10}$$

where

$$\begin{cases} s_k = Cx_k \\ \delta_k = \sqrt{x_k^T P_2 x_k} \end{cases} \tag{11}$$

i.e. s_k is a linear function of x_k and C satisfies $C^T C = P_1$. Moreover, if $\mathrm{rank}(P_2) = \mathrm{rank}(P_1) = 1$, δ_k is a linear function of x_k too, i.e.

$$\delta_k = Dx_k$$

and D satisfies $D^T D = P_2$.

The following theorem shows that this simplified form of the PR-sliding sector does exist for controllable plants.

Theorem 2. *For any controllable plant described by eqn. (1), there exist two linear functions s_k and δ_k of x_k*

$$s_k = Cx_k, \qquad C = \begin{bmatrix} c_1 & c_2 & \dots & c_n \end{bmatrix} \in \mathbb{R}^{1\times n}$$

$$\delta_k = Dx_k, \qquad D = \begin{bmatrix} d_1 & d_2 & \dots & d_n \end{bmatrix} \in \mathbb{R}^{1\times n}$$

such that the PR-sliding sector defined by (4) or (6) can be rewritten as a simplified form.

Proof. For a controllable system, there exists an invertible transformation T

$$x_k = Tz_k$$

which transforms (1) to the controllable canonical form

$$z_{k+1} = \bar{\Phi}z_k + \bar{\Gamma}u_k$$

where

$$\bar{\Phi} = T^{-1}\Phi T = \begin{bmatrix} 0 & 1 & \cdots & 0 \\ \vdots & \vdots & \ddots & \vdots \\ 0 & 0 & \cdots & 1 \\ -a_0 & -a_1 & \cdots & -a_{n-1} \end{bmatrix}$$

$$\bar{\Gamma} = T^{-1}\Gamma = \begin{bmatrix} 0 & \cdots & 0 & 1 \end{bmatrix}^T$$

Let $\tilde{P}$ be the $n\times n$ identity matrix and $\tilde{R}$ be the $n\times n$ zero matrix. Then the PR-sliding sector is determined by

$$\begin{aligned} x_k^T(\Phi^T P\Phi - P + R)x_k &= z_k^T(\bar{\Phi}^T\tilde{P}\bar{\Phi} - \tilde{P} + \tilde{R})z_k \\ &= \Big\{(a_0-1)z_1 + a_1z_2 + \cdots + a_{n-1}z_n\Big\} \\ &\times \Big\{(a_0+1)z_1 + a_1z_2 + \cdots + a_{n-1}z_n\Big\} \\ &= z_k^T\bar{C}^T\bar{C}z_k - z_k^T\bar{D}^T\bar{D}z_k \\ &= s_k^2 - \delta_k^2 \le 0 \end{aligned}$$

where

$$\begin{aligned} P &= T^{-T}\tilde{P}T^{-1} \\ R &= T^{-T}\tilde{R}T^{-1} \\ s_k &= \bar{C}z_k = \begin{bmatrix} a_0 & a_1 & \dots & a_{n-1} \end{bmatrix} z_k \\ \delta_k &= \bar{D}z_k = \begin{bmatrix} 1 & 0 & \dots & 0 \end{bmatrix} z_k \end{aligned}$$

It follows that if $P = (TT^T)^{-1}$ and $R = O_n$, then the PR-sliding sector can be defined as

$$\mathcal{S} = \left\{ x_k \middle| \ |s_k| \leq |\delta_k| \right\}$$

where

$$s_k = Cx_k, \qquad C = \bar{C}T^{-1}$$

$$\delta_k = Dx_k, \qquad D = \bar{D}T^{-1}$$

This completes the proof. ■

2.2. Design of PR-Sliding Sectors Using the Riccati Equation

In the proof of Theorem 2, a PR-sliding sector has been designed for the controllable canonical form. Now we shall design a PR-sliding sector using a Riccati equation.

For the plant (1), the performance index is chosen as

$$J = \sum_{k=0}^{\infty} (x_k Q x_k^T + u_k^2) \tag{12}$$

where $Q \in \mathbb{R}^{n \times n}$ is a positive-definite symmetric matrix.

Since (Φ, Γ) is controllable, the optimal control minimizing (12) exists and has the form

$$u_k = -Kx_k \tag{13}$$

where the gain matrix K is defined as

$$K = (1 + \Gamma^T P \Gamma)^{-1} \Gamma^T P \Phi \tag{14}$$

and $P \in \mathbb{R}^{n \times n}$ is a positive-definite symmetric matrix which satisfies the following discrete-time Riccati equation:

$$P = Q + \Phi^T P \Phi - \Phi^T P \Gamma (1 + \Gamma^T P \Gamma)^{-1} \Gamma^T P \Phi \tag{15}$$

By substituting (13) into (1), the closed-loop system yields

$$x_{k+1} = (\Phi - \Gamma K) x_k \tag{16}$$

If a solution P of (15) is chosen so as to define the P-norm in Definition 1, then

$$\begin{aligned} L_{k+1} - L_k &= x_k^T (\Phi^T P \Phi - P) x_k \\ &= x_k^T K^T (1 + \Gamma^T P \Gamma) K x_k - x_k^T Q x_k \end{aligned} \tag{17}$$

with zero control input.

The following theorem concludes how to design a PR-sliding sector using the Riccati equation.

Theorem 3. *If the solution P of the discrete-time Riccati equation is used to define the P-norm and $R = 0$, then the PR-sliding sector (4) can be rewritten as*

$$\mathcal{S} = \left\{ x_k \middle| \ |s_k| \leq |\delta_k| \right\} \tag{18}$$

where

$$s_k = Cx_k, \qquad C = \sqrt{1 + \Gamma^T P \Gamma}\, K \tag{19}$$

$$\delta_k = \sqrt{x_k^T Q x_k} \tag{20}$$

Q is the matrix in the performance index (12), K is the optimal feedback-gain matrix determined by (14).

Proof. According to (17), the following equation holds when $u_k = 0$:

$$\begin{aligned} L_{k+1} - L_k &= x_k^T (\Phi^T P \Phi - P) x_k \\ &= x_k^T K^T (1 + \Gamma^T P \Gamma) K x_k - x_k^T Q x_k \\ &= s_k^2 - \delta_k^2 \end{aligned}$$

Therefore, (18) defines a simplified PR-sliding sector. ∎

2.3. VS Controller

For the sliding sector (10), a VS control law should be designed to move the system state from the outside to the inside of the PR-sliding sector. Inside the PR-sliding sector, the P-norm keeps decreasing. For discrete-time systems, the system state, in general, may not stay inside the PR-sliding sector forever when there is no control action. Thus the VS control law will be used again to move the system state from the outside to the inside of the PR-sliding sector. While the system state is moving in such a way, the P-norm may increase for some plants. To design a discrete-time VS controller with the PR-sliding sector, this sector was redesigned in (Furuta and Pan, 1996) to ensure that the P-norm decreases after a finite number of initial steps.

In this paper, a new VS control law is proposed for sampled-data systems. The discrete-time system (1) is considered as a sampled-data system of the continuous-time one

$$\dot{x}(t) = Ax(t) + Bu(t) \tag{21}$$

with sampling interval T. Then

$$\Phi = e^{AT}, \qquad \Gamma = \int_0^T e^{At} B \, \mathrm{d}t$$

Theorem 4. *For the discrete-time plant (1) with the PR-sliding sector (18) designed by using the Riccati equation, the discrete-time VS control law*

$$u_k = \begin{cases} 0 & \text{if} \quad x_k \in \mathcal{S} \\ -(C\Gamma)^{-1}(C\Phi x_k - \beta s_k) & \text{if} \quad x_k \bar{\in} \mathcal{S} \end{cases} \tag{22}$$

stabilizes the system if

1. *the coefficient* β *satisfies* $|\beta| < 1$,
2. *the discrete-time plant (1) is a sampled-data system of (21) with sampling interval* T, *and*
3. *there exist a sufficiently small* T, *a coefficient* β, *and positive constants* λ_i $(i = 1, 2, 3$ *and* $\lambda_1 + \lambda_2 + \lambda_3 = 1)$ *such that*

$$C\Gamma > 0 \tag{23}$$

$$\lambda_1 2\sqrt{1+h}(1-\beta) > C\Gamma \tag{24}$$

$$\lambda_2^2(1-\beta)^2 Q > T^2 H^T(T) H(T) \tag{25}$$

$$2\sqrt{1+h}\lambda_3 > h(C\Gamma)^{-1}(1-\beta)(1+\lambda_2)^2 \tag{26}$$

where Q *is the positive-definite symmetric matrix used to design the PR-sliding sector,*

$$H(T) = C\sum_{n=1}^{\infty} \frac{A^n}{n!} T^{n-1}, \qquad h = \Gamma^T P \Gamma$$

Proof. It will be shown that the P-norm decreases in the whole state space.

First, consider the inside of the PR-sliding sector. In this case, we have $s_k^2 \leq \delta_k^2$ and the P-norm decreases with the VS control law (22) because

$$\begin{aligned} L_{k+1} - L_k &= x_{k+1}^T P x_{k+1} - x_k^T P x_k \\ &= s_k^2 - \delta_k^2 \leq 0 \end{aligned}$$

Now consider the outside of the PR-sliding sector, i.e. the case $s_k^2 > \delta_k^2$. With the VS control law (22), we obtain

$$s_{k+1} = C x_{k+1} = C\Phi x_k + C\Gamma u_k = \beta s_k$$

i.e.

$$s_{k+1}^2 = \beta^2 s_k^2 < s_k^2$$

Thus the system state will move toward the inside of the PR-sliding sector. At the same time, from (14) and (19), we see that

$$\begin{aligned} L_{k+1} - L_k &= x_{k+1}^T P x_{k+1} - x_k^T P x_k \\ &= x_k^T(\Phi^T P \Phi - P) x_k + 2\sqrt{1+h}\, s_k u_k + h u_k^2 \\ &= s_k^2 - \delta_k^2 + 2\sqrt{1+h}\, s_k u_k + h u_k^2 \\ &= s_k(s_k + 2\sqrt{1+h}\, u_k) + h u_k^2 - \delta_k^2 \end{aligned}$$

If there exist λ_i ($\lambda_i > 0$, $i = 1,2,3$ and $\lambda_1 + \lambda_2 + \lambda_3 = 1$), a coefficient β, and a sufficiently small sampling interval T such that (23)–(26) hold, then

$$\begin{aligned}
|u_k| &= (C\Gamma)^{-1}|(1-\beta)s_k + TH(T)x_k| \\
&\leq (C\Gamma)^{-1}\Big\{(1-\beta)|s_k| + \sqrt{T^2 x_k^T H^T(T)H(T)x_k}\Big\} \\
&\leq (C\Gamma)^{-1}\Big\{(1-\beta)|s_k| + \sqrt{\lambda_2^2(1-\beta)^2 x_k^T Q x_k}\Big\} \\
&= (C\Gamma)^{-1}\Big\{(1-\beta)|s_k| + \lambda_2(1-\beta)|\delta_k|\Big\} \\
&< (C\Gamma)^{-1}|s_k|(1-\beta)(1+\lambda_2)
\end{aligned}$$

and

$$\begin{aligned}
L_{k+1} - L_k &< s_k(s_k + 2\sqrt{1+h}\,u_k) + h(C\Gamma)^{-2}s_k^2(1-\beta)^2(1+\lambda_2)^2 - \delta_k^2 \\
&= (C\Gamma)^{-1}s_k\Big\{\big(C\Gamma - 2\sqrt{1+h}(1-\beta)\big)s_k - 2\sqrt{1+h}\,TH(T)x_k\Big\} \\
&\quad + h(C\Gamma)^{-2}s_k^2(1-\beta)^2(1+\lambda_2)^2 - \delta_k^2 \\
&< -(C\Gamma)^{-1}2\sqrt{1+h}\Big\{(1-\beta)(1-\lambda_1)s_k^2 + s_k TH(T)x_k\Big\} \\
&\quad + h(C\Gamma)^{-2}s_k^2(1-\beta)^2(1+\lambda_2)^2 - \delta_k^2 \\
&< -(C\Gamma)^{-1}2\sqrt{1+h}(1-\beta)\lambda_3 s_k^2 + h(C\Gamma)^{-2}s_k^2(1-\beta)^2(1+\lambda_2)^2 - \delta_k^2 \\
&< -\delta_k^2 < 0
\end{aligned}$$

Therefore the discrete-time VS control law (22) ensures that the state moves toward the inside of the PR-sliding sector and the P-norm decreases in the whole state space, which implies that the proposed VS controller stabilizes the system (1) or (21). ■

Remark 2. The conditions (23)–(26) are satisfied for a small sampling interval T.

3. Experimental Apparatus

The overview of the rotational inverted pendulum is shown in Fig. 1. The pendulum has an additional dynamics between the link and the housing which holds the axis of the hinge. The sole actuator is a Direct-Drive motor which can torque the arm with a possible range of -9.8 to 9.8 [Nm]. We can measure angles of the motor and pendulum using encoders whose possible range is from $0°$ to $360°$ with the resolution of 102400 [pulse/rev] and 4096 [pulse/rev], respectively.

The additional dynamics consists of a mass, springs and dumpers. It is introduced as the uncertainty of the pendulum system.

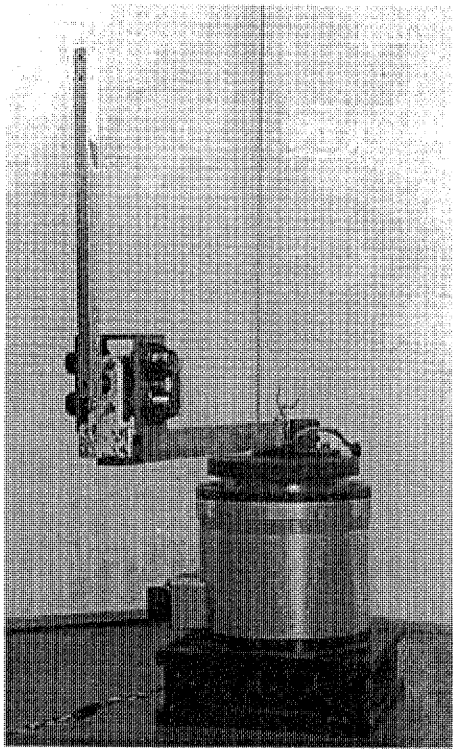

Fig. 1. Rotational inverted pendulum.

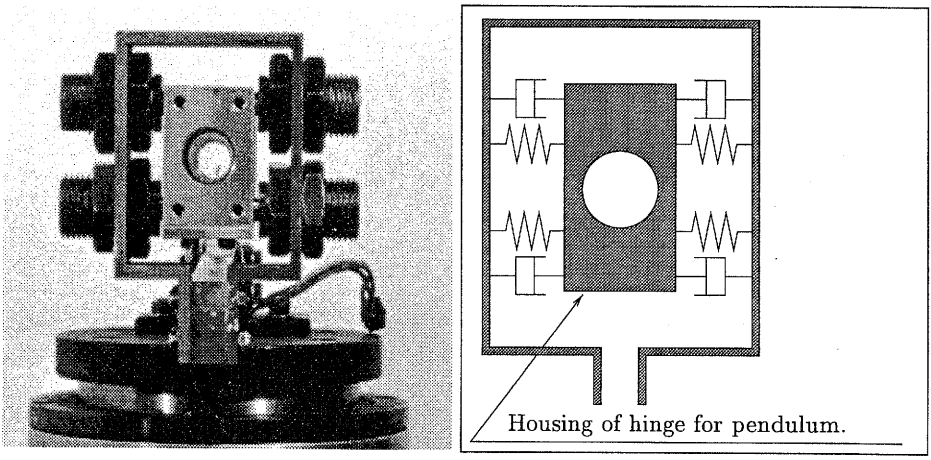

Fig. 2. Additional dynamics.

Figure 3 shows the configuration of the system with the additional dynamics. All the parameters of the configuration are given according to the DH-notation (Denavit and Hartenberg, 1955). All the controllers are designed based on the nominal model which does not include the additional dynamics. The configuration of the nominal model is shown in Fig. 4.

Table 1. DH parameters of Fig. 3.

Link	a	α	d	θ
1	a_1	$-\pi/2$	0	θ_1
2	0	$\pi/2$	δ_2	$\pi/2$
3	a_3	0	0	θ_3

Table 2. DH parameters of Fig. 4.

Link	a	α	d	θ
1	0	$\pi/2$	0	θ_1
2	a_2	0	d_2	θ_2

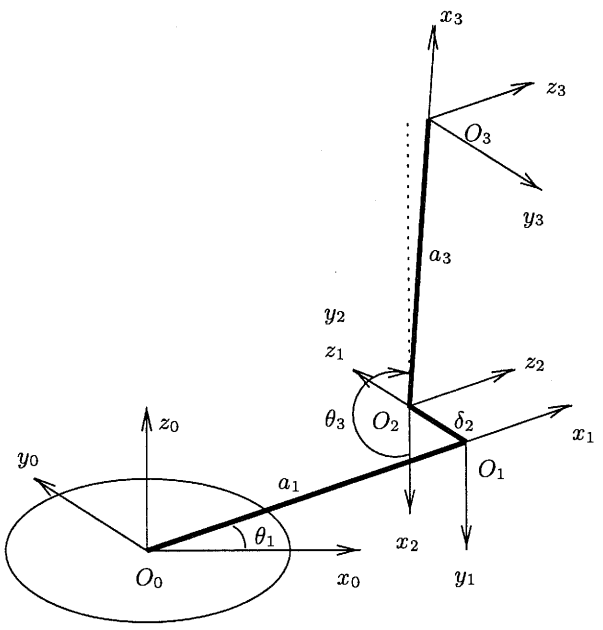

Fig. 3. Configuration of the system with additional dynamics.

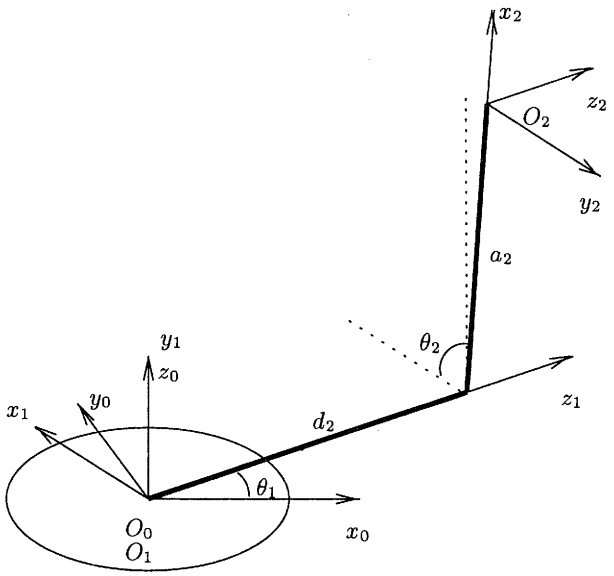

Fig. 4. Configuration of the system without additional dynamics.

The dynamic equations for the system with the additional dynamics are as follows:

$$
\begin{aligned}
&V_1\ddot{q}_1 + 2(a_3 + s_{3x})m_3 \sin(q_3)\dot{\delta}_2\dot{q}_1 \\
&\quad + 2(m_2 + m_3)\delta_2\dot{\delta}_2\dot{q}_1 + 2m_3(J_{3y} - J_{3x})\cos(q_3)\sin(q_3)\dot{q}_1\dot{q}_3 \\
&\quad + 2m_3(a_3 + s_{3x})^2 \cos(q_3)\sin(q_3)\dot{q}_1\dot{q}_3 + 2m_3(a_3 + s_{3x})\cos(q_3)\delta_2\dot{q}_1\dot{q}_3 \\
&\quad - (a_3 + a_{3x})a_1 m_3 \sin(q_3)\dot{q}_3^2 + (m_2 + m_3)a_1\ddot{\delta}_2 \\
&\quad + \left(J_{1y} + J_{2x} + J_{3x} + a_1^2(m_2+m_3) + m_1(a_1+s_{1x})^2\right)\ddot{q}_1 + (J_{3y} - J_{3x})\sin^2(q_3)\ddot{q}_1 \\
&\quad + m_3(a_3 + s_{3x})^2 \sin^2(q_3)\ddot{q}_1 + 2m_3(a_3 + s_{3x})\sin(q_3)\delta_2\ddot{q}_1 + (m_2 + m_3)\delta_2^2\ddot{q}_1 \\
&\quad + m_3(a_3 + s_{3x})a_1 \cos(q_3)\ddot{q}_3 = \tau
\end{aligned}
$$

$$
\begin{aligned}
&K_2\delta_2 + V_2\dot{\delta}_2 - (a_3 + s_{3x})m_3 \sin(q_3)\dot{q}_1^2 - (m_2 + m_3)\delta_2\dot{q}_1^2 - m_3(a_3 + s_{3x})\sin(q_3)\dot{q}_3^2 \\
&\quad + (m_2 + m_3)\ddot{\delta}_2 + a_1(m_2 + m_3)\ddot{q}_1 m_3(a_3 + s_{3x})\cos(q_3)\ddot{q}_3 = 0
\end{aligned}
$$

$$
\begin{aligned}
&(a_3 + s_{3x})gm_3 \sin q_3 + (J_{3x} - J_{3y})\cos(q_3)\sin(q_3)\dot{q}_1^2 \\
&\quad - (a_3 + s_{3x})^2 m_3 \cos(q_3)\sin(q_3)\dot{q}_1^2 - (a_3 + s_{3x})m_3 \cos(q_3)\delta_2\dot{q}_1^2 + V_3\dot{q}_3 \\
&\quad + (a_3 + s_{3x})m_3 \cos(q_3)\ddot{\delta}_2 + (a_3 + s_{3x})a_1 m_3 \cos(q_3)\ddot{q}_1 \\
&\quad + J_{3z}\ddot{q}_3 + (a_3 + s_{3x})^2 m_3\ddot{q}_3 = 0
\end{aligned}
$$

The corresponding parameters are listed in Table 3.

Table 3. Parameters of dynamic equations for the system with additional dynamics

g	9.81 [m/s^2]	acceleration of gravity
a_1	0.195 [m]	length of link
a_3	0.205 [m]	length of pendulum
m_1	2.63 [kg]	mass of link and rotor
m_2	0.45 [kg]	mass of additional dynamics
m_3	0.15 [kg]	mass of pendulum
J_{1y}	0.0266 [kg m^2]	moment of inertia around center of gravity of link
J_{2x}	0 [kg m^2]	moment of inertia around center of gravity of additional dynamical system
J_{3x}	0.0000025 [kg m^2]	moment of inertia around x_3 axis of pendulum
J_{3y}	0.000527 [kg m^2]	moment of inertia around y_3 axis of pendulum
J_{3z}	0.000527 [kg m^2]	moment of inertia around z_3 axis of pendulum
s_{1x}	-0.156 [m]	length from point to center of gravity of link
s_{3x}	-0.1025 [m]	length from point to center of gravity of pendulum
V_1	0.0308 [kg/s]	coefficient of viscosity around rotation axis
V_2	144.0 [kg/s]	coefficient of viscosity in additional dynamics
V_3	0.0033235 [kg/s]	coefficient of viscosity around hinge for pendulum
K_2	1372 [kg/s^2]	coefficient of the additional dynamics in springs

The dynamic equations for the system without the additional dynamics are as follows:

$$
\begin{aligned}
&V_1\dot{q}_1 + (J_{2x} + J_{2y})\sin(2q_2)\dot{q}_1\dot{q}_2 - m_2(a_2 + s_{2x})^2\sin(2q_2)\dot{q}_1\dot{q}_2 \\
&\quad - m_2(a_2 + s_{2x})d_2\cos(q_2)\dot{q}_2 + \left(J_{1y} + J_{2y} + m_2(a_2 + s_{2x})^2 + m_2 d_2^2 + m_1 s_{1x}^2\right)\ddot{q}_1 \\
&\quad + \left(J_{2x} + J_{2y} + m_2(a_2 + s_{2x})^2\right)\sin^2(q_2)\ddot{q}_1 \\
&\quad + m_2(a_2 + s_{2x})d_2\sin^2(q_2)\ddot{q}_2 = \tau
\end{aligned}
$$

$$
\begin{aligned}
&m_2(a_2 + s_{2x})g\cos(q_2) + (J_{2y} - J_{2y})\cos(q_2)\sin(q_2)\dot{q}_1^2 \\
&\quad + m_2(a_2 + s_{2x})^2\cos(q_2)\sin(q_2)\dot{q}_1^2 + V_2\dot{q}_2 - m_2(a_2 + s_{2x})d_2\sin(q_2)\ddot{q}_1 \\
&\quad + (J_{2z} + m_2(a_2 + s_{2x})^2)\ddot{q}_2 = 0
\end{aligned}
$$

and the corresponding parameters are given in Table 4.

Table 4. Parameters of dynamic equations of the system without additional dynamics

g	9.81 [m/s^2]	acceleration of gravity
a_2	0.205 [m]	length of pendulum
d_2	0.195 [m]	length of link
m_1	3.08 [kg]	mass of link and motor
m_2	0.15 [kg]	mass of pendulum
J_{1y}	0.0266 [kg m^2]	moment of inertia around center of gravity about link
J_{2x}	0.0000025 [kg m^2]	moment of inertia around x_2 axis of pendulum
J_{2y}	0.000527 [kg m^2]	moment of inertia around y_2 axis of pendulum
J_{2z}	0.000527 [kg m^2]	moment of inertia around z_3 axis of pendulum
s_{1z}	0.039404 [m]	length from point to center of gravity of link
s_{2x}	-0.1025 [m]	length from point to center of gravity of pendulum
V_1	0.0308 [kg/s]	coefficient of viscosity around rotation axis
V_2	0.0033235 [kg/s]	coefficient of viscosity around hinge for pendulum

By linearizing the above equations around the unstable equilibrium state, the state equations of each model are obtained as follows. For the system with additional dynamics we have

$$\dot{x} = Ax + bu$$

where

$$A = \begin{pmatrix} 0 & 0 & 0 & 1 & 0 & 0 \\ 0 & 0 & 0 & 0 & 1 & 0 \\ 0 & 0 & 0 & 0 & 0 & 1 \\ 0 & 8742.36 & 0 & -1.00645 & 917.565 & 0 \\ 0 & -4518.6 & 2.26161 & 0.196257 & -474.255 & -0.0498344 \\ 0 & -20572.5 & 88.258 & 0 & -2159.22 & -1.94476 \end{pmatrix}$$

$$b = \begin{pmatrix} 0 & 0 & 0 & 32.6768 & -6.37198 & 0 \end{pmatrix}^T$$

$$x = \begin{pmatrix} q_1 & \delta_2 & q_3 & \dot{q_1} & \dot{\delta_2} & \dot{q_3} \end{pmatrix}^T$$

q_1 is the angle of the link, δ_2 stands for the displacement of the hinge, q_3 denotes the angle of the pendulum.

The system without additional dynamics has the parameters

$$A = \begin{pmatrix} 0 & 0 & 1 & 0 \\ 0 & 0 & 0 & 1 \\ 0 & 6.5531 & -0.938621 & -0.144397 \\ 0 & 81.0655 & -1.33818 & -1.78627 \end{pmatrix}$$

$$b = \begin{pmatrix} 0 & 0 & 30.4747 & 43.4473 \end{pmatrix}^T$$

$$x = \begin{pmatrix} q_1 & q_2 & \dot{q}_1 & \dot{q}_2 \end{pmatrix}^T$$

where q_1 is the angle of the link and q_2 denotes the angle of the pendulum.

Discretizing the above nominal continuous system with the sampling time $T = 0.005\,\mathrm{s}$ gives the following discrete-time system:

$$x_{k+1} = \Phi x_k + \Gamma u_k$$

where

$$\Phi = e^{AT}$$

$$\Gamma = \int_0^T e^{At} b \, \mathrm{d}t$$

$$\Phi = \begin{pmatrix} 1 & 8.15565 \times 10^{-5} & 4.98829 \times 10^{-3} & -1.66101 \times 10^{-6} \\ 0 & 1.00101 & -1.66543 \times 10^{-5} & 4.97942 \times 10^{-3} \\ 0 & 3.25541 \times 10^{-2} & 9.95320 \times 10^{-1} & -6.35770 \times 10^{-4} \\ 0 & 4.03550 \times 10^{-1} & -6.64773 \times 10^{-3} & 9.92118 \times 10^{-1} \end{pmatrix}$$

$$\Gamma = \begin{pmatrix} 3.80216 \times 10^{-4} \\ 5.40723 \times 10^{-4} \\ 1.51944 \times 10^{-1} \\ 2.15835 \times 10^{-1} \end{pmatrix}$$

The Bode diagrams of both systems are compared in Figs. 5 and 6.

4. Results of Experiment

An experiment has been carried out to stabilize the pendulum with discrete-time VSC and LQ-optimal controller. For comparison, both the controllers were designed based on the nominal model with the same positive definite solution P of the Riccati equation (15) with two different state weight matrices Q. The observers were designed based on Gopinath's method. The poles which were used for designing the observer are 0.9 for the LQ optimal controllers and 0.58 for the discrete-time VS controllers.

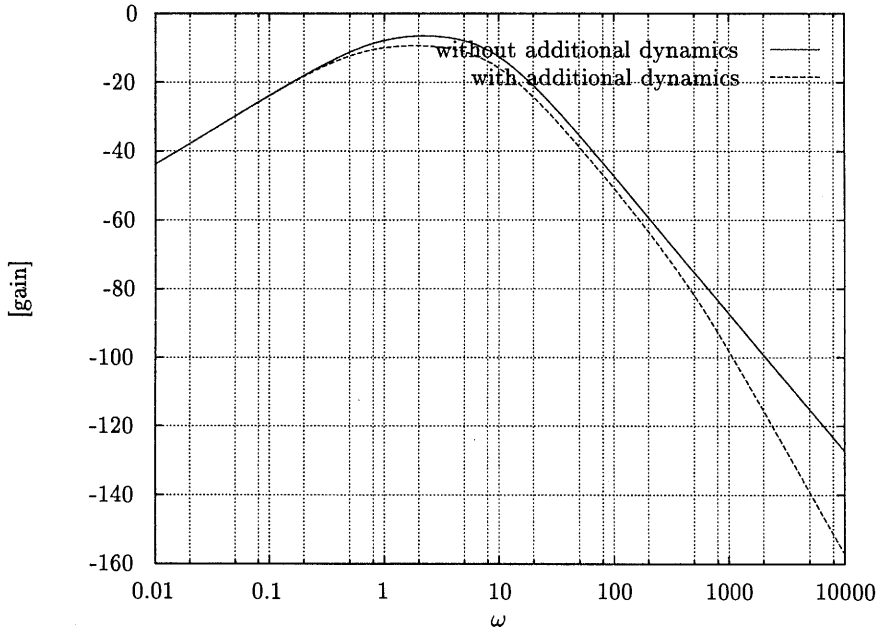

Fig. 5. Gain of the frequency characteristic from the input to the angle of the pendulum.

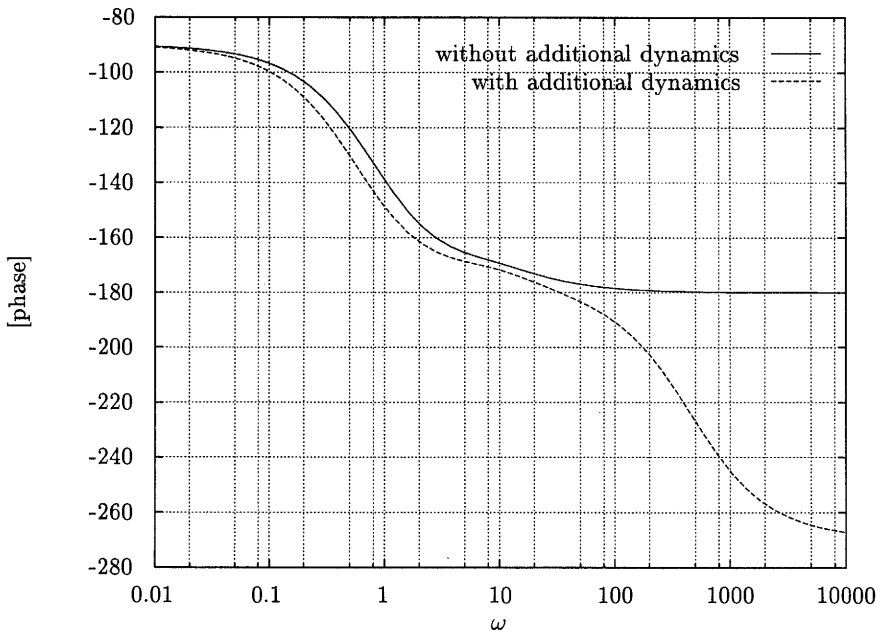

Fig. 6. Phase of the frequency characteristic from the input to the angle of the pendulum.

The fast observer does not work satisfactorily for the LQ optimal controllers. Figures 7–11 show the response of the pendulum system. The spike-like responses are due to disturbances which were added to test the robustness of the system to disturbances.

First, we choose the matrix Q of the performance index (12) as

$$Q = \begin{pmatrix} 100000 & 0 & 0 & 0 \\ 0 & 10000 & 0 & 0 \\ 0 & 0 & 2000 & 0 \\ 0 & 0 & 0 & 1000 \end{pmatrix} \triangleq Q_1 \tag{27}$$

Equation (15) gives the positive-definite solution P as

$$P = \begin{pmatrix} 8.50444 \times 10^6 & -1.06489 \times 10^7 & 1.58666 \times 10^6 & -1.12023 \times 10^6 \\ -1.06489 \times 10^7 & 2.26194 \times 10^7 & -3.14612 \times 10^6 & 2.23578 \times 10^6 \\ 1.58666 \times 10^6 & -3.14612 \times 10^6 & 4.59980 \times 10^5 & -3.25012 \times 10^5 \\ -1.12023 \times 10^6 & 2.23578 \times 10^6 & -3.25012 \times 10^5 & 2.31689 \times 10^5 \end{pmatrix}$$

which yields the LQ optimal control law

$$u_k = -Kx_k$$

where

$$K = \begin{pmatrix} -3.09884 \times 10^1 & 1.27218 \times 10^2 & -1.32081 \times 10^1 & 1.40149 \times 10^1 \end{pmatrix}^T$$

Accordingly, the parameters C and Q of (18) are determined as

$$C = \begin{pmatrix} -3.16153 \times 10^2 & 1.29792 \times 10^3 & -1.34753 \times 10^2 & 1.42984 \times 10^2 \end{pmatrix}^T$$

$$Q = Q_1$$

and the coefficient β of the VS control law (22) is chosen to be 0.8 in the experiment.

Figures 7 and 8 show the responses of the angle $q_2 - \pi/2$ of the pendulum for the discrete-time VSC and the LQ-optimal control, respectively. The discrete-time VSC reveals a quicker response against the disturbance than the LQ-optimal controller. Figures 9 and 10 show the input torque around z_0 for the discrete-time VSC and the LQ-optimal control, respectively. As can be seen, the input of the discrete-time VSC requires a larger torque than that of the LQ-optimal control. Figure 11 is zooming up Fig. 9 with the time range from 6 to 10 seconds. One can observe that the VS controller produces a zero input while the state of the system stays within the sliding sector.

It is experimentally observed that the system with the LQ optimal controller may lose stability when the feedback coefficient K is large due to a large value of Q and starts slugging motion in the presence of the uncertain model dynamics. Next, we conduct experiments with a large value of the matrix Q.

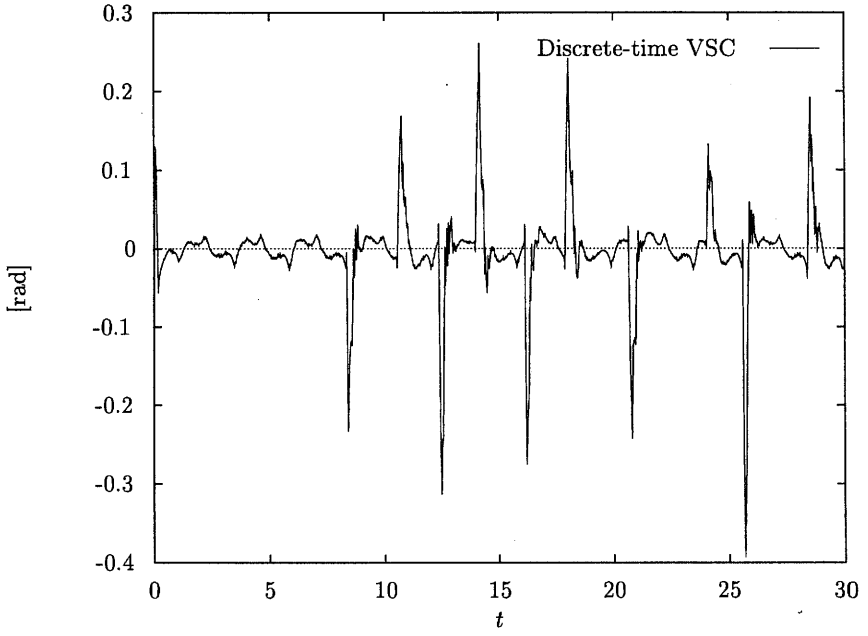

Fig. 7. Response with discrete-time VS controller based on Q_1.

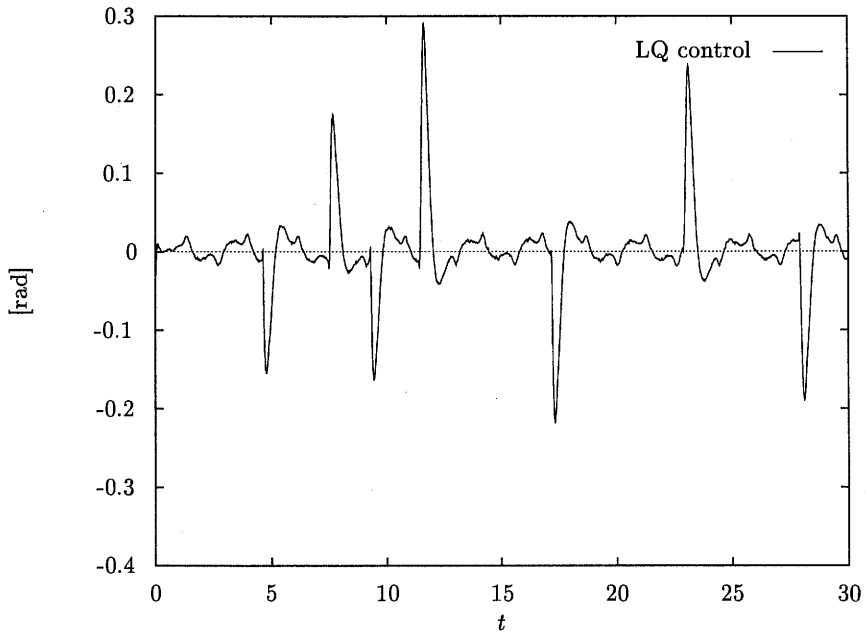

Fig. 8. Response with LQ optimal controller based on Q_1.

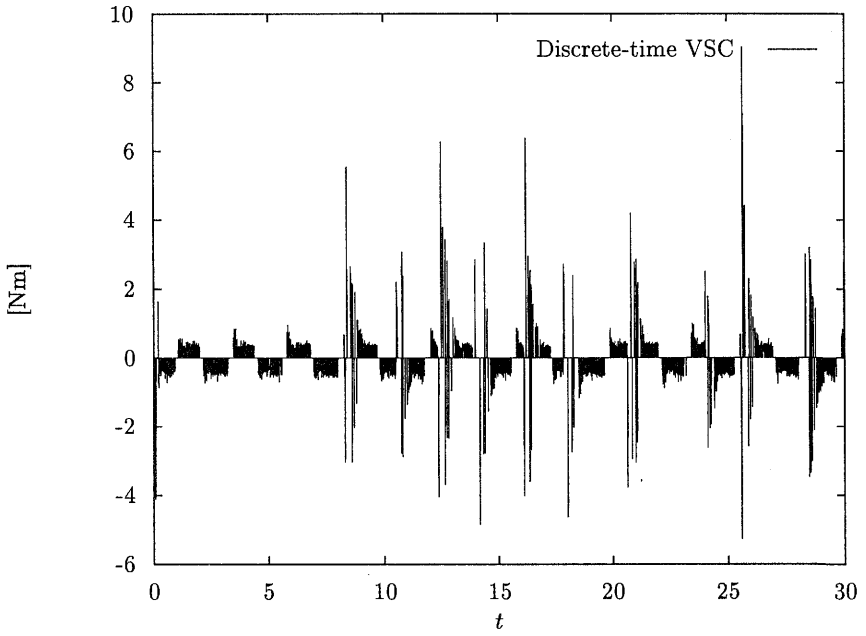

Fig. 9. Input with discrete-time VS controller based on Q_1.

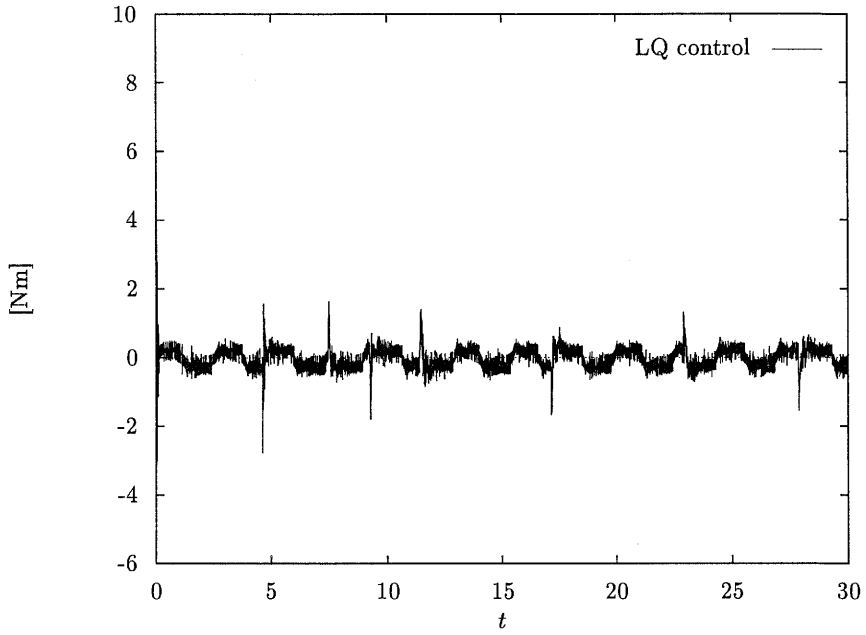

Fig. 10. Input with LQ optimal controller based on Q_1.

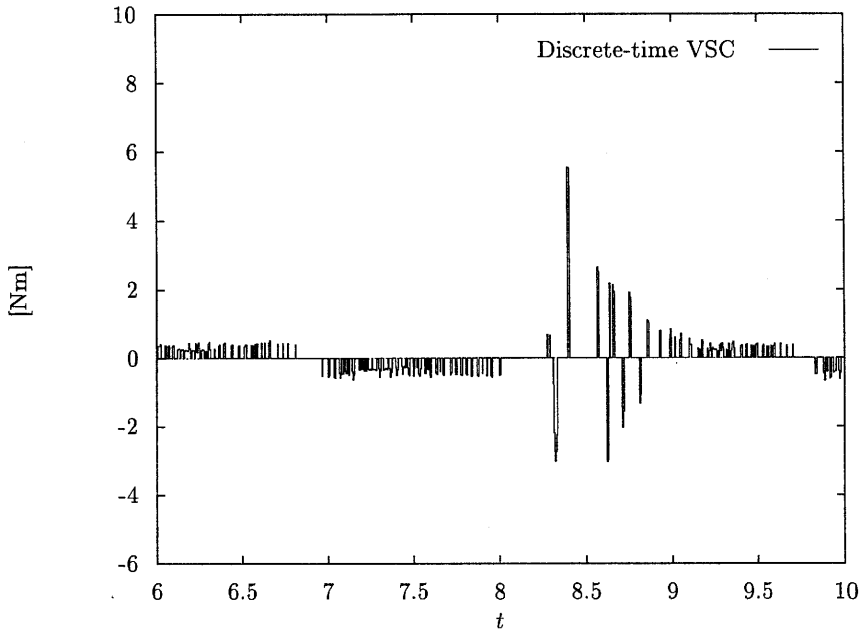

Fig. 11. Zooming up of input with discrete-time VS controller.

The matrix Q of the performance index (12) is chosen this time as

$$Q = \begin{pmatrix} 1000000 & 0 & 0 & 0 \\ 0 & 10000 & 0 & 0 \\ 0 & 0 & 2000 & 0 \\ 0 & 0 & 0 & 1000 \end{pmatrix} \triangleq Q_2 \tag{28}$$

Equation (15) gives the positive-definite solution P as

$$P = \begin{pmatrix} 6.51056 \times 10^7 & -6.63872 \times 10^7 & 1.00840 \times 10^7 & -7.09730 \times 10^6 \\ -6.63872 \times 10^7 & 8.43934 \times 10^7 & -1.25280 \times 10^7 & 8.84589 \times 10^6 \\ 1.00840 \times 10^7 & -1.25280 \times 10^7 & 1.88516 \times 10^6 & -1.32908 \times 10^6 \\ -7.09730 \times 10^6 & 8.84589 \times 10^6 & -1.32908 \times 10^6 & 9.39088 \times 10^5 \end{pmatrix}$$

which yields the LQ optimal control law

$$u_k = -Kx_k$$

where

$$K = \begin{pmatrix} -9.77095 \times 10^1 & 2.45969 \times 10^2 & -3.09902 \times 10^1 & 2.66170 \times 10^1 \end{pmatrix}^T$$

Accordingly, the parameters C and Q of the PR-sliding sector (18) are determined as

$$C = \left(-1.02632 \times 10^3 \quad 2.58361 \times 10^3 \quad -3.25515 \times 10^2 \quad 2.79579 \times 10^2\right)^T$$

$$Q = Q_2$$

the coefficient β of the VS control law (22) is chosen to be 0.8 in the experiment.

Figures 12 and 13 show the responses of the angle $q_2 - \pi/2$ of the pendulum for the discrete-time VSC and the LQ-optimal control, respectively. In contrast to the slugging response with the LQ optimal control, there does not exist the slugging motion in the response with the discrete-time VSC and the discrete-time VSC gives a quicker response against the disturbances. Figures 14 and 15 show the control inputs for the discrete-time VSC and the LQ-optimal control, respectively. From these figures, we can observe that the discrete-time VSC gives a better input to the system than the LQ optimal controller.

5. Conclusion

In this paper, the discrete-time VSC based on the sliding sector is evaluated by the newly proposed pendulum system with additional dynamics. From the results of the experiment, we can conclude that the discrete-time VSC with the sliding sector designed by using the same criterion for the Riccati equation gives a faster response against disturbances than the LQ optimal control. The discrete-time VSC can incorporate a high gain with which the LQ optimal controller may start the slugging motion.

References

Furuta K. (1990): *Sliding mode control of a discrete system.* — Syst. Contr. Lett., Vol.14, No.2, pp.145–152.

Furuta K. and Pan Y. (1993): *VSS controller design for discrete-time system.* — Proc. IEEE Int. Conf. *Industrial Electronics, Control, and Instrumentation*, Hawaii, Vol.3, pp.1950–1955.

Furuta K. and Pan Y. (1994): *Discrete-time VSS control for continuous-time system.* — Proc. 1st *Asian Contr. Conf.*, Tokyo, pp.377–380.

Furuta K. and Pan Y. (1995): *A new approach to design a sliding sector for VSS controller.* — Proc. *Amer. Contr. Conf.*, Seattle, pp.1304–1308.

Furuta K. and Pan Y. (1996): *Design of discrete-time VSS controller based on sliding sector.* — Proc. 13th IFAC *World Congress*, Vol.F, pp.487–492.

Iordanou H.N. and Surgenor B.W. (1997): *Experimental evaluation of the robustness of discrete sliding mode control versus linear quadratic control.* — IEEE Trans. Contr. Syst. Techn., Vol.5, No.2, pp.254–260.

Denavit J. and Hartenberg R.S. (1955): *A kinematics notation for lower pair mechanism.* – J. Applied Mechanics, Vol.22, No.2, pp.215–221.

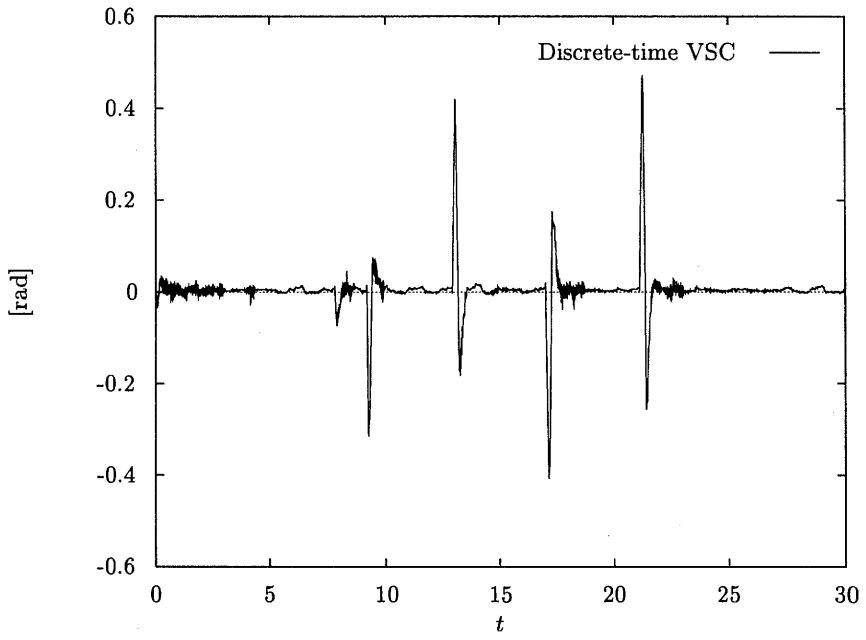

Fig. 12. Response with discrete-time VS controller based on Q_2.

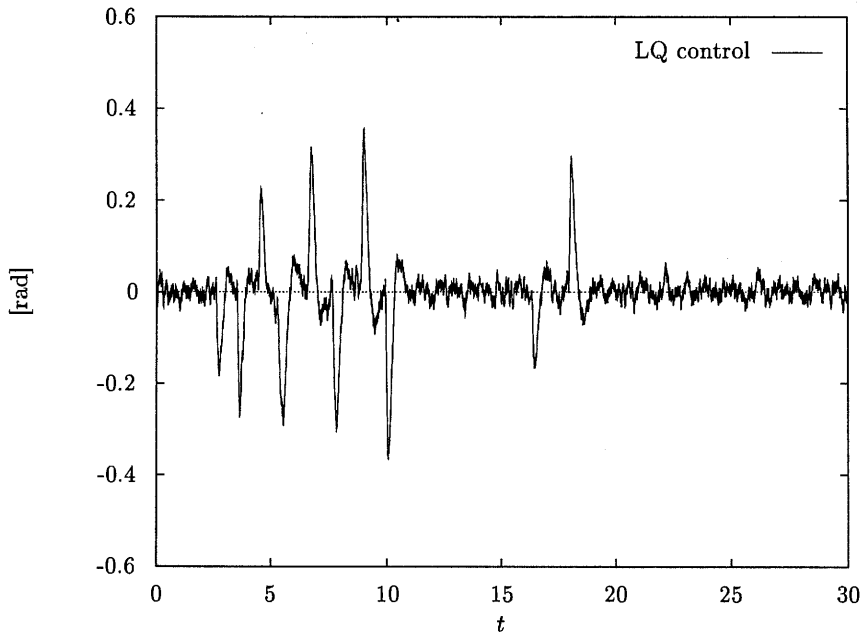

Fig. 13. Response with LQ optimal controller based on Q_2.

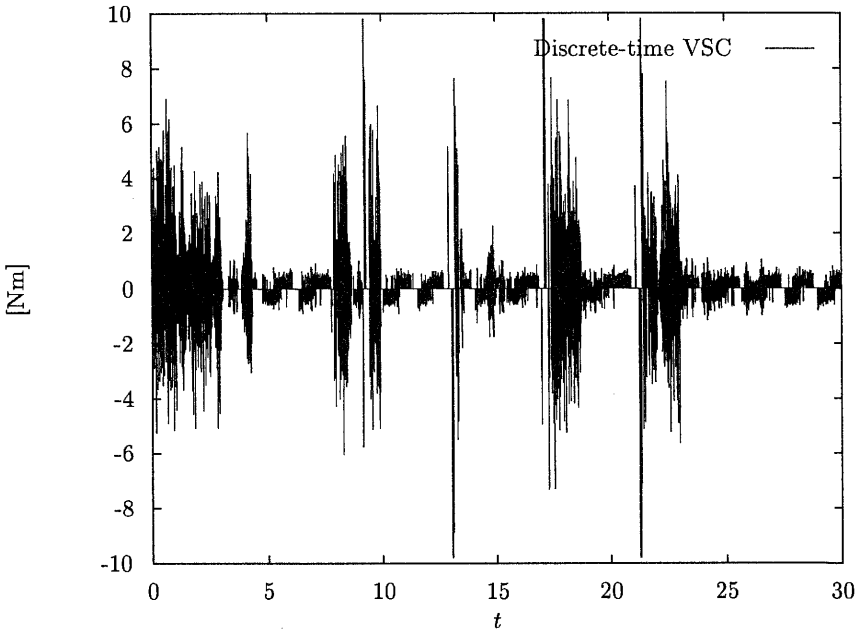

Fig. 14. Input with discrete-time VS controller based on Q_2.

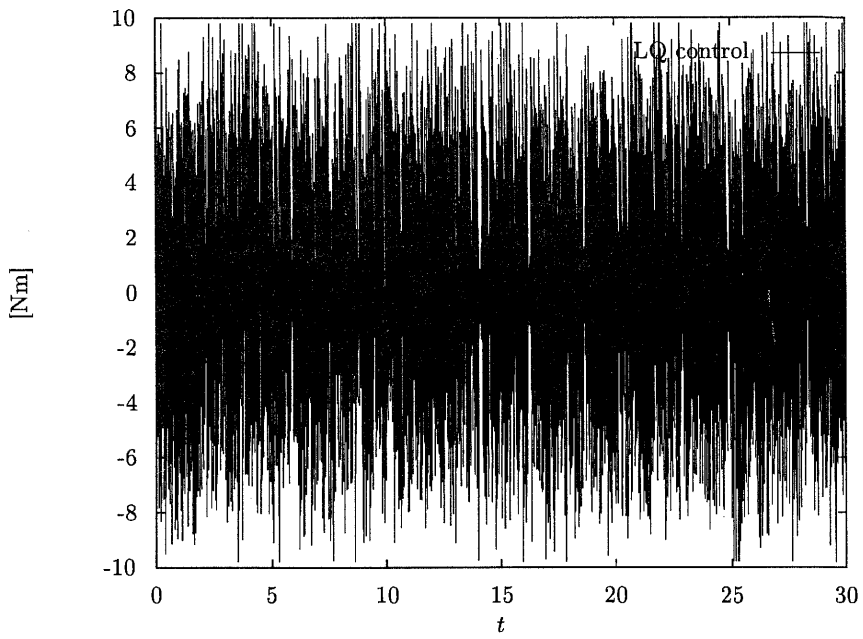

Fig. 15. Input with LQ optimal controller based on Q_2.